International Conference on Applied Energy 2019
Aug 12-15, 2019, Västerås, Sweden
Paper ID: 1079

A MANUFACTURING METHOD FOR LARGE-DIMENSION LATTICE TRUSS PANEL STRUCTURE USED IN HIGH-EFFICIENT COMPACT HEAT EXCHANGER

Shaohua Li[1], Wenchun Jiang[1,*], Xuefang Xie[1],Jian Li[2], Bin Yang[1]

1. State Key Laboratory of Heavy Oil Processing, College of Chemical Engineering, China University of Petroleum (East China), Qingdao, 266580, PR China

2. Key Laboratory of Neutron Physics and Institute of Nuclear Physics and Chemistry, China Academy of Engineering Physics, Mianyang 621999, PR China

(Corresponding author: jiangwenchun@126.com)

ABSTRACT

The mechanical characteristics of 304 stainless steel T-joint and lattice truss panel structure with pyramidal core were extensively investigated by the combinational methods of the experiments, finite element simulation and analytical model. The experimental results reveal that a T-joint with 2.25kW laser welding power, 2.5m/min welding speed and 5mm separation performs the better ultimate tensile load and strength ratio. The mechanical responses of T-joints are mainly dominated by elastic-plastic deformations. The laser welding reduces slightly the elasticity, ultimate tensile strength and fracture toughness of the structure. The joints present typical ductile fracture once the loads reach fracture strength. Under three-point bending test, the mechanical curve is divided into elastic, yield and failure region, and the deformation characterizes and failure modes are tension and shearing stress controlling. The results are verified by the FEM simulation.

Keywords: laser welding, lattice truss panel structure, mechanical properties, high-efficient compact heat exchanger

NONMENCLATURE

Abbreviations	
APEN	Applied Energy
Symbols	
n	Year

1. INTRODUCTION

Lattice truss panel structure (LTPS) has the advantages of lightweight, high strength and high efficiency of heat transfer. It has an promising potential in application in compact heat exchangers at high temperature gas reactor (HTGR) and modern steam turbine. The PLTPS fabrication method by laser welding is widely recognized as a kind of advanced connection technology whose application prospect is very broad [1-4]. It is essential to investigate the mechanical and fracture properties [5-7] of the T-joints due to that plenty of T-joints are arranged in the junction which influences the structural integrity significantly and the deformation characteristics and failure mode of the PLTPS.

As the weakest part of the entire components [8], and the strength of T-joint affects the integrity of the overall structure seriously. Last decades, abundant researches have reported the effects of welding process and defects caused by manufacturing process on the formation [9,10] and mechanical properties [11,12] of the T-joints. Mikko Jutila [13] studied the micro-failure behavior of the T-joint under uniaxial tension and the failure mode and mechanism. The deformation responses of T-joint are mainly divided into metal yield, plastic deformation. Xiong [14] clarified the bending failure mode and the effect of welding parameters on the bending properties of the T-joints. The lightweight

Selection and peer-review under responsibility of the scientific committee of the 11th Int. Conf. on Applied Energy (ICAE2019).

design, fabrication [15,16], mechanical behavior [17–19] and multifunctional application [20–24] of the LTPS have been widely investigated. The combinational methods including experimental, finite element analysis and theoretical model have been used to study the mechanical properties and failure modes of this structure

Plenty of researches have concentrated on manufacturing technology and simple properties and failure mode, detailed correlation between deformation feature, while failure behavior is still not clear and required to be extensively studied. In this study, firstly, a series of welding experiments were performed to select the optimal welding process parameters. Then, the deformation characteristics and fracture modes of the welding T-joints were identified by the load-displacement curves and microstructure analysis. Finally, the finite element simulation of the three-point bending and analytical models were employed to analysis the deformation characteristics and failure behavior of the PLTPS.

2. FABRICATION METHOD OF T-JOINT AND PLTPS BY LASER WELDING

Analyzing the macro-morphology of the welds, a part of welding process parameter is determined: the deflection angle is 5°, the protection gas with flux is 20L/min is the high-purity argon gas. The effect of welding powers and welding speeds on the properties of the joints are investigated furtherly and the parameters details are shown in Table 1. The cylindrical hourglass polished specimens with a parallel length of 150mm and a width of 30mm were designed and machined in accordance with the requirement of ASME standards E606-2004. A fixture is added on the side-faces of the specimen to ensure the tightness coefficient of the web plate and face plate. The detailed specimen dimension is shown in Fig. 1.

Table 1 The welding process parameter details

No.	Power （kW）	Speed （m/min）	Separation (mm)
1	2.0	2.5	+5
2	2.5	3.0	+5
3	2.25	2.5	+5
4	2.0	2.5	+3
5	1.8	2.5	+3
6	2.0	3.0	+3
7	1.8	3.0	+3

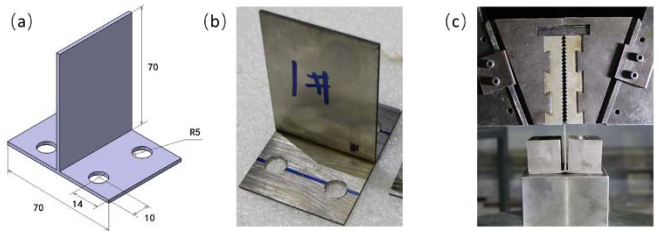

Fig.1 The schematic of the dimension of T-joint and assembly

The PLTPS is a periodic structure, which consists two face plates and lattice pyramidal unit-cell. Figure (2) exhibits preparation dimension of horizontal and longitudinal lattice unit-cell. The face plates and periodic unit-cell are prepared by superhigh-pressure water cutting machine, firstly. Secondly, corresponding fillister joints are prefabricated to ensure the interference fitting and assembled to prevent the relative rotation between longitudinal and horizontal unit-cells. Then, the face plates and lattice pyramidal core are constrained in the laser welding machine by two fixtures that are added on the side upper- and lower- face plates to ensure the tightness coefficient of the trusses and plates. Finally, one group of process parameter is employed to weld the PLTPS. It is proposed that the longitudinal cores are welded firstly, and the horizontal welding is conducted from the middle to sides sequentially. This method reduces the effects of the clamping gap between the core and the panel.

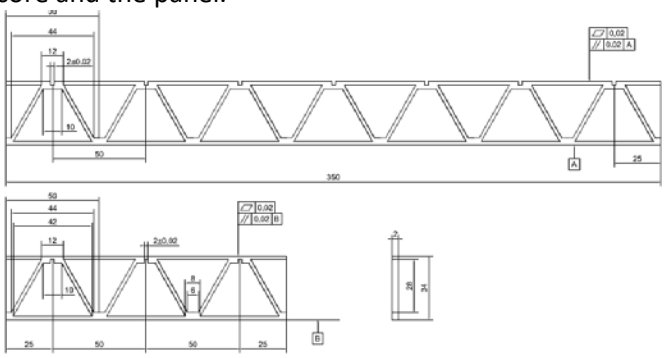

Fig. 2 The dimension of horizontal and longitudinal lattice unit-cell

3 FINITE ELEMENT SIMULATION

T-joints were assembled to MTS servo-hydraulic machine and loaded constant tensile velocity of 1mm/min. The test is interrupted until the final fracture of the specimen. In order to clarify the mechanical response and failure mode of the LTPS, the corresponding 3D finite element mode is established, which consists of 21unit-cells arranged in 7×3. The C3D8 element type is adopted in this simulation and the effect of the element numbers on calculation results is examined. There are 1,815,401 nodes and 1,538,412 elements are meshed.

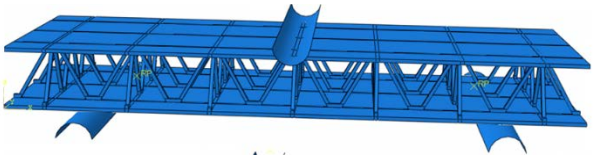

Fig. 3 The FEM simulation models

4 RESULTS

The mechanical curves for the T-joints welded by different process parameters are shown in Fig.4. An obvious linear-elastic performance is observed until reaching the ultimate point. The maximum and minimum elastic modulus are 157.2 and 128.2GPa. However, the specimen fracture instantaneously when the tested load exceeds ultimate load, which is significantly different with the load-displacement curve of the base metal that presences a yield region. In addition, the curves of the T-joint absent obvious hardening region.

The macro-morphology of the T-joint is exhibited in Fig. 5. It is obvious that the welds are divided into heat affected zone (HAZ) and melting zone by the fusion line. The undercooling of the weld edge is larger due to the faster cooling rate of the laser welding process. As a result, the crystal near the fusion line is mostly growth in a dendritic form. The dendrite growth from weld boundary to the weld center, and the growth direction is perpendicular to the fusion line. Since the center weld cooling with low rate, the center of the weld is mainly equiaxed crystals with uniform distribution. The equiaxed crystals filled in the weld center are smaller and more compact than the dendrite near the fusion zone, the weld strength is improved significantly.

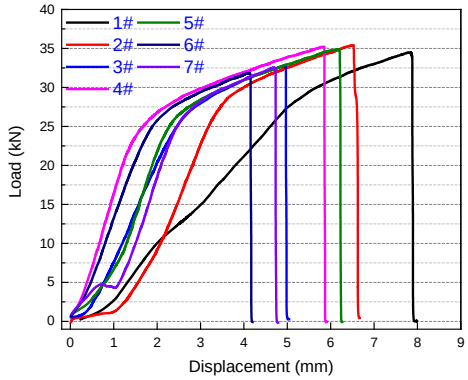

Fig.4 The load-displacement curves of the T-joints

Table 2 The welding process parameter details

No.	Ultimate load（kN）	Ultimate strength (MPa)	Strength radio (%)
1	36.15	454.717	87.45
2	37.45	471.0692	90.59
3	37.94	477.2327	91.77
4	35.51	446.6667	85.89
5	35.00	440.2516	84.66
6	33.76	424.6541	81.66
7	32.67	410.9434	79.028

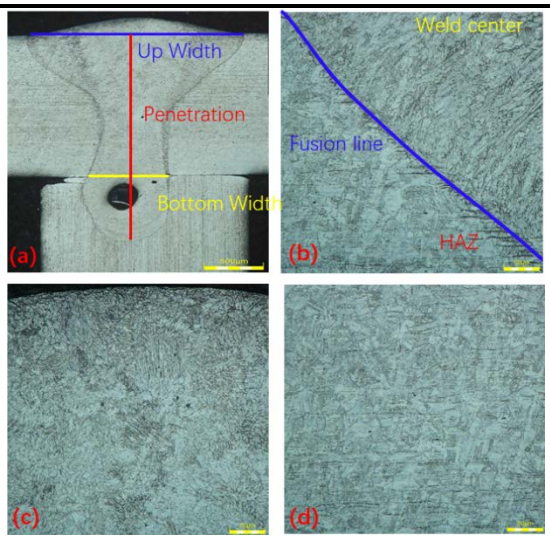

Fig. 5 The macro-morphology of characteristic dimensions (a), fusion zone (b), center weld (c) and base metal (d)

5 DISCUSION

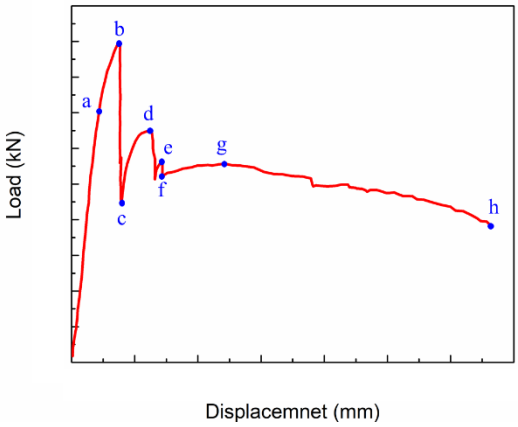

Fig. 6 The characteristic curve of three-point bending test

The characteristic mechanical response curve of the lattice material under three-point load is shown in Fig. 6. The load increases linearly with the increase of displacement at near-linear elastic state (*oa*). It implies that the pyramidal lattice materials mainly produce elastic deformation when deflection is small. And the yield of materials is not obvious before the load research ultimate load. The plastic collapse strength was derived as follow:

The load rapidly reaches the yield limit (point b) with the increase of displacement. The curve drops sharply when the localized truss buckle at *bc* state, and which increases the effective stress shared on the remaining trusses and reduces the compression resistance of the lattice material significantly. The

deformation mode transforms from bending to coupling of bending-shearing. At *cd* state, it is clarified that the material is reinforced due to that the deflected truss contacts to the plate, which is similar to the yield character and reaches a second peak load at point d. The joints bear greater coupling bend-shearing stress which is mainly caused by incongruous deformation of the cores and plates and the different failure. Under the complex stress distribution, the gap between cores and face plate is identified as crack-source that results in surface-core debond and the mechanical properties curve decreases correspondingly. The surface-core debond are also found in ab state, however, the effect of debond failure can be ignored. At *gh* state, the material deforms consecutively and truss rupture until the test is interrupted.

To further reveal the cyclic mechanical properties and failure modes of the LTPS, the stress distribution of the structure is extensively analyzed. Figure (7) describe the stress contours of the LTPS at different period. It is clearly that the elasticity dominants the deformation of the core and face plate when the loaded displacement is limited. While the deformation modes of the center and side cores are different, i.e. the trusses of the center core are mainly compressed, and the shearing stress are imposed on the trusses of the side cores. In this case, the effective elastic and shearing models and the critical buckling stress of the LTPS are derived.

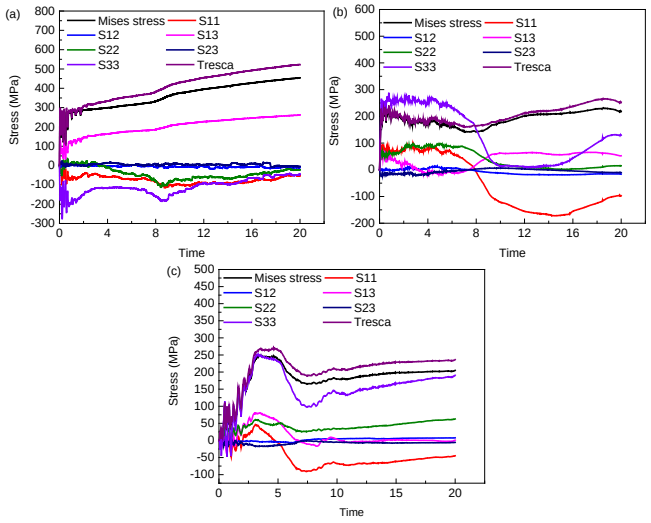

Fig.7 The FEM results

Figure 8 presents the anisotropic stress of the center (a), nearby (b) and side (c) core. It reveals that the trusses suffer from complex stress, i.e. tension and shear coupling stress dominants the deformation and failure modes. For the center core, both the compressive stress (S33) and shearing stress (S13) are greater than the other direction stress when the deflection is small. It is obvious the S33 decreases significantly when the truss buckles. Then the controlling stress transforms from coupling stress to shearing stress. While, the S11 and S33 play major roles in the deformation of the trusses in nearby and side cores.

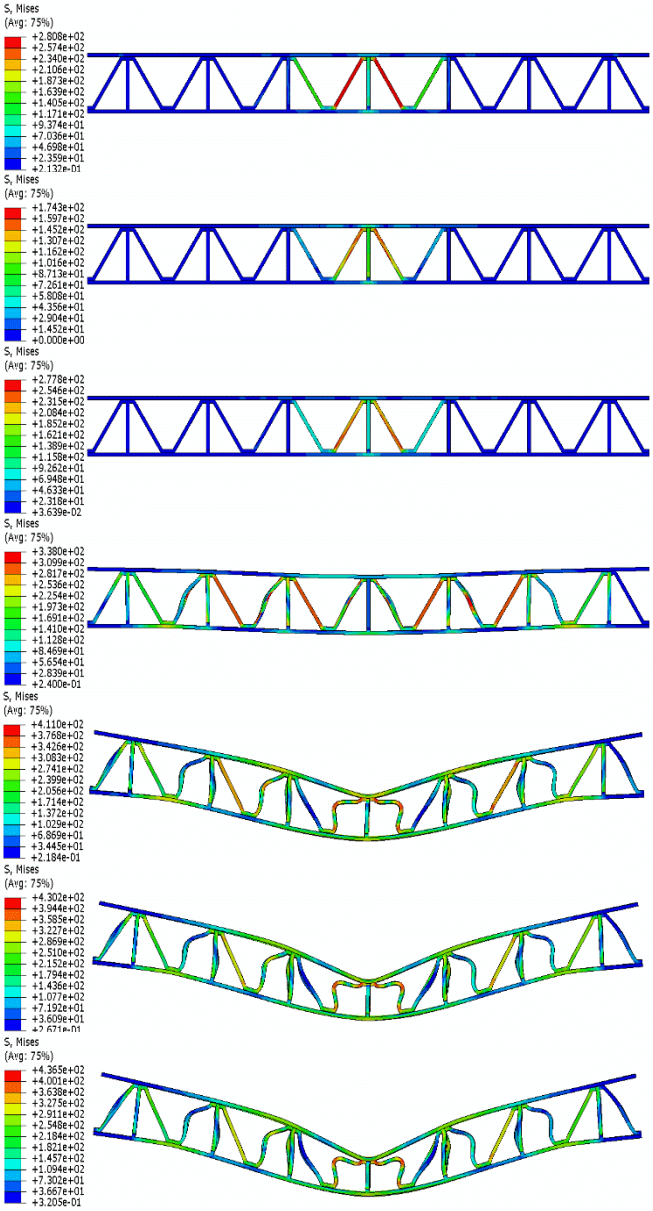

Fig.8 The FEM results

6 CONCLUSION

In this study, the mechanical properties and failure mode of LTPS were investigated by experiment, FEM and analytical methods. T-joints was manufactured by the selected welding parameters. In addition, the tension tests of the T-joints were conducted. The main conclusions are listed as follows:

(1) The maximum ultimate tensile load is obtained by the T-joints with 2.25kW laser welding power, 2.5m/min welding speed and 5mm separation.

(2) The mechanical properties of T-joints are mainly dominanted by elastic-plasitc deformations, and the strength of the weld is very close to the strength of the base metal. The T-joints present mimetic brittle when the loads reach fracture strength.

(3) Under three-point bending load, the LTPS presents elastic deflection, face wrinkle, truss buckling, plastic deformation, face-core debonded and truss rupture, respectively.

ACKNOWLEDGEMENT

The authors gratefully acknowledge the support provided by National Natural Science Foundation of China (11372359 and 51575531), Taishan Scholar Construction Funding (ts201511018) and Fundamental Research Funds for the Central Universities (17CX05019).

REFERENCE

[1]. Chen YB, Cao LJ. State of the study of laser welding of Aluminum alloys. Weld Jo 2001;03:9-12

[2] Lavernia EJ, Srivatsan TS, Mohamed FA. Strength, deformation, fracture behaviour and ductility of aluminium-lithium alloys. J Mater Sci 1990;25:1137–1158.

[3] Srivatsan TS, Sudarshan TS. Welding of lightweight aluminum lithium alloys. Weld Jo 1991;70:173-185

[4] Ravindra A, Dwarakadasa ES, Srivatsan TS, Ramanath C, Iyengar K. Electron-beam weld microstructures and properties of aluminium-lithium alloy 8090. J Mater Sci 1993;28:3173–3182.

[5] Acherjee B. Hybrid laser arc welding: State-of-art review. Opt Laser Technol 2018;99:60-71

[6] Ha J, Huh H. Failure characterization of laser welds under combined loading conditions. Int J Mech Sci 2013;69:40-58

[7] Zhu MF, Lu FG, Chen YX, Yao Y. Finite element analysis on laser welding of aluminum alloy. Transaction of the China welding Institution 2008;29:97-100.

[8] Chen Y, Jiang X. Cao Y, et al. Study of laser welding method and mechanical properties on T-joint of sandwich structure. Hot Working Technology. 2014;1:173~175.

[9] Li G, Liu L. Investigation on weld ability of magnesium alloy thin sheet T-joints: arc welding, laser welding and laser-arc hybrid welding. Int J Adv Manuf Tech 2013;65:27~34.

[10] Romanoff J, Reddy JN. Experimental validation of the modified couple stress Timoshenko beam theory for web-core sandwich panels. Compos Struct 2014;111:130~137.

[11] Meng W, Li Z, Huang J, Wu Y. Effect of gap on plasma and molten pool dynamics during laser lap welding for T-joints. Int J Adv Manuf Tech 2013;69:1105~1112.

[12] Kutsuna M, Yan Q. Study on porosity formation in laser welds in aluminium alloys (Report 1): Effects of hydrogen and alloying elements. Weld In 1998;12:937-949.

[13] Mikko J. Failure Mechanism of a Laser Stake Welded T-Joint. Ph.D. Thesis, Helsinki University of Technology, 2009.

[14] Xu X, Qiao JS, Jiang X, Zhu L, Wu YX, Chen JH. Study on Bending Behavior of Laser Welding T Joints of 960 High Strength Steel. Hot Working Technology 2044;19:158~161.

[15] Fricke W, Robert C, Peters R, Sumpf A. Fatigue strength of laser-stake welded T-joints subjected to combined axial and shear loads. Welding in the World 2016;60:593-604.

[16] Li WX, Sun F, Wang P, Fan HL, Fang DN. A novel carbon fiber reinforced lattice truss sandwich cylinder: fabrication and experiments. Compos Part A 2016;81:313–22.

[17] Queheillalt Douglas T, Murty Yellapu, Wadley Haydn NG. Mechanical properties of an extruded pyramidal lattice truss sandwich structure. Scripta Mater 2008;58:76–9.

[18] Yin Sha, Wua Linzhi, Maa Li, Nutt Steven. Pyramidal lattice sandwich structures with hollow composite trusses. Compos Struct 2011;93:3104–11.

[19] Finnegan K, Kooistra G, Wadley HNG, Deshpande VS. The compressive response of carbon fiber composite pyramidal truss sandwich cores. Int J Mater Res 2007;98:1264–72.

[20] Xiong J, Ma L, Pan S, Wu L, Papadopoulos J, Vaziri A. Shear and bending performance of carbon fiber composite sandwich panels with pyramidal truss cores. Acta Mater 2012;60:1455–66.

[21] Liu H, Zhang HW. An equivalent multiscale method for 2D static and dynamic analyses of lattice truss materials. Adv Eng Softw 2014;75:14–29.

[22] Lu TJ, Valdevit I, Active Evans AG. Cooling by metallic sandwich structures with periodic cores. Prog Mater Sci 2005;50:789–815.

[23] Tian J, Lu TJ, Hodson HP, Queheillalt DT, Wadley HNG. Cross flow heat exchange of textile cellular

metal core sandwich panels. Int J Heat Mass Transfer 2007;50:2521–36.
[24] Queheillalt Douglas T, Carbajal Gerardo, Peterson GP, Wadley Haydn NG. A multifunctional heat pipe sandwich panel structure. Int J Heat Mass Transfer 2008;51:312–26.